Bone 123 (2019) 28–38

Contents lists available at ScienceDirect

Bone

journal homepage: www.elsevier.com/locate/bone

Full Length Article

Oral dosing of pentoxifylline, a pan-phosphodiesterase inhibitor restores bone mass and quality in osteopenic rabbits by an osteogenic mechanism: A comparative study with human parathyroid hormone

Subhashis Pal[a], Konica Porwal[a], Kunal Khanna[b], Manoj Kumar Gautam[c], Mohd Yaseen Malik[d], Mamunur Rashid[d], R. John Macleod[e], Muhammad Wahajuddin[d], Venkitanarayanan Parameswaran[c], Jayesh R. Bellare[b], Naibedya Chattopadhyay[a,*]

[a] Division of Endocrinology, CSIR-Central Drug Research Institute, Council of Scientific and Industrial Research, Lucknow 226031, India
[b] Department of Chemical Engineering, Indian Institute of Technology-Bombay, Mumbai 400076, India
[c] Department of Mechanical Engineering, Indian Institute of Technology-Kanpur, Kanpur 208016, India
[d] Division of Pharmaceutics, CDRI-CSIR, Lucknow 226031, India
[e] Department of Biomedical and Molecular Sciences, Queen's University, Kingston, Ontario, Canada

ARTICLE INFO

Keywords:
Pharmacokinetics
Bone turnover
Bone quality
Bone formation
Bone resorption
Osteopenia

ABSTRACT

The non-selective phosphodiesterase inhibitor pentoxifylline (PTX) is used for the treatment of intermittent claudication due to artery occlusion. Previous studies in rodents have reported salutary effects of the intraperitoneal administration of PTX in segmental bone defect and fracture healing, as well as stimulation of bone formation. We determined the effect of orally dosed PTX in skeletally mature ovariectomized (OVX) rabbits with osteopenia. The half-maximal effective concentration (EC_{50}) of PTX in rabbit bone marrow stromal cells was 3.07 ± 1.37 nM. The plasma PTX level was 2.05 ± 0.522 nM after a single oral dose of 12.5mg/kg, which was one-sixth of the adult human dose of PTX. Four months of daily oral dosing of PTX at 12.5 mg/kg to osteopenic rabbits completely restored bone mineral density, bone mineral content (BMC), microarchitecture and bone strength to the level of the sham-operated (ovary intact) group. The bone strength to BMC relationship between PTX and sham was similar. The bone restorative effect of PTX was observed in both axial and appendicular bones. In osteopenic rabbits, PTX increased serum amino-terminal propeptide, mineralized nodule formation by stromal cells and osteogenic gene expression in bone. PTX reversed decreased calcium weight percentage and poor crystal packing found in osteopenic rabbits. Furthermore, similar to parathyroid hormone (PTH), PTX had no effect on bone resorption. Taken together, our data show that PTX completely restored bone mass, bone strength and bone mineral properties by an anabolic mechanism. PTX has the potential to become an oral osteogenic drug for the treatment of post-menopausal osteoporosis.

1. Introduction

Post-menopausal osteoporosis occurs due to increased bone resorption over bone formation, leading to net bone loss and increased risk of fracture [1,2]. Daily injection of teriparatide, the N-terminal part of human parathyroid hormone (PTH) and a modified version of parathyroid hormone-related protein (PTHrP) are clinically used osteoanabolic therapies that primarily act by directly stimulating osteoblasts in addition to other indirect mechanisms [3]. Orally active osteoanabolic therapy is an unmet medical need. A recent study showed that 67% of patients in the USA discontinue teriparatide by the end of the first year following initiation [4]. In general, treatment adherence and persistence are greater with oral over perenteral modes of drug administration [5]. Consequently an oral osteoanabolic drug is preferred.

PTH and PTHrP act on osteoblasts by stimulating the parathyroid hormone 1 receptor (PTH1R), a class B G protein-coupled receptor (GPCR) to increase levels of intracellular cAMP [6]. This rise in cAMP then activates the cAMP responsive element binding protein (CREBP) to upregulate osteogenic transcription factors Runx-2 and osterix. [7]. Elevated cAMP is a required upstream event in the osteogenic cascade displayed not only by PTH but also by β-adrenergic agonists [8] as well as TSH (thyroid stimulating hormone) [9].

Another way to increase intracellular cAMP is to inhibit the

* Corresponding author at: Endocrinology Division, CSIR-Central Drug Research Institute, Lucknow 226021, India.
E-mail address: n_chattopadhyay@cdri.res.in (N. Chattopadhyay).

https://doi.org/10.1016/j.bone.2019.03.010
Received 29 August 2018; Received in revised form 6 March 2019; Accepted 8 March 2019
Available online 09 March 2019

phosphodiesterases (PDE) responsible for its degradation [10]. As such, it is reasonable to speculate that increasing cAMP in osteoblasts to levels comparable to stimulation by PTH using PDE inhibition might result in an osteoanabolic effect similar to PTH. Pentoxifylline (PTX) is a non-selective PDE inhibitor that is used orally for the treatment of peripheral arterial occlusive disease [11]. There are reports that intraperitoneal injection (IP) of PTX influence fracture healing in some models. In rats, repair of a critical-sized segmental defect made in the radius diaphysis was promoted by IP administration of PTX at 25 mg/kg [12]. PTX given at 100 mg/kg, also by IP administration, showed an increasing trend in bending stiffness in osteopenic rats with femur osteotomy [13]. In growing mice, the daily subcutaneous injections of PTX (100–200 mg/kg) demonstrated increases in both cortical and trabecular bone mass by promoting bone formation [14]. These studies suggest an osteogenic potential of PTX, albeit when administered by parenteral routes. PTX has been used for the past several decades in the symptomatic management of intermittent claudication thereby attesting to its safety [15]. Consequently, evidence of skeletal restoration by this drug in an osteopenic animal model by an osteogenic mechanism would strongly suggest its use in post-menopausal osteoporosis without the need for a multitude of safety studies in animals and humans normally required for new chemical entities. Therefore, we set out to determine the osteogenic effect of PTX in osteopenic rabbits.

In the current study, osteopenic rabbits were used since unlike rats and mice, rabbits possess active Haversian remodeling and achieve skeletal maturity quickly [16]. As described herein, we determined the minimum osteogenic dose by pharmacokinetic studies. Then, in skeletally mature rabbits where bone remodeling is the dominant event [17] [18], we tested the skeletal response of orally administered PTX in an osteopenic rabbit model by assessing bone mass, microarchitecture, bone formation, bone turnover, bone strength and bone quality in comparison with subcutaneously injected PTH (1–34).

2. Materials and methods

2.1. Reagents and chemicals

Cell culture media, collagenase, and all fine chemicals were purchased from Sigma-Aldrich (St. Louis, MO, USA) while cell culture supplements including FBS and diaspase were purchased from Invitrogen (Carlsbad, CA, USA). PTX was purchased from Sigma-Aldrich and human PTH (1–34) was purchased from Neobiolab (Cambridge, MA, USA).

2.2. Animals and experimental procedures

All animal experimental procedures were prior approved (Institutional Animal Ethics Committee approval no. CDRI/IAEC/2015/132) and conducted as per the guidelines laid by the Committee for the Purpose of Control and Supervision of Experiments on Animals (CPCSEA), Ministry of Environment and Forests, Government of India. New Zealand White (NZW) rabbits used for the study were obtained from the National Laboratory Animal Centre, CSIR-CDRI. Rabbits (one per cage) were housed in temperature controlled (22–24 °C) rooms having fresh air supply with 100% exhaust air to the outside and 60–70% relative humidity. Rooms had diffuse lighting in the range of 200–300 lx and equipped for automatic maintenance of a diurnal 12 h light cycle. Rabbits were fed ad libitum with lucerne grass and maintenance diet (Nutrilab, Provimi, Chennai, India) and had free access to RO water.

For ovariectomy (OVX) and sham surgery, anesthesia was induced with xylazine (3 mg/kg) and ketamine (20 mg/kg). Post-operatively all rabbits were administered with antibiotic enrofloxacin (6.5 mg/kg, intramuscular 2× daily) for the first 7 days and analgesic meloxicam (0.2 mg/kg, intramuscular daily) for the first 3 days.

2.3. In vitro studies

2.3.1. ALP assay

For osteoblast differentiation of bone marrow stromal cells (BMSC), bone marrow cells were harvested from the femur of adult female rabbits and 4×10^4 cells/well were seeded into 24-well plates using 10% FBS containing α-MEM to obtain adherent cells following our previously published protocol [19]. These cells were treated with PTX (range, 10^{-11} M–10^{-6} M) for 48 h in ALP induction medium (α-MEM supplemented with 10 mM β-glycerophosphate and 50 μg/ml ascorbic acid). 1,25-$(OH)_2$ vitamin D_3 (10 nM) was used as a positive control. 2 mg/ml para-Nitrophenylphosphate (pNPP) in diethanolamine buffer (DAE) was used to measure ALP activity calorimetrically at 405 nm.

2.3.2. Mineralization assay

BMSCs were cultured as described above having seeding density of 2×10^6 cells/well in the osteogenic differentiation medium (α-MEM with 10 mM β-glycerophosphate, 50 μg/ml ascorbic acid, and 100 nM dexamethasone) with or without PTX (3 nM) for 16 days with the change in medium every 48 h. Mineralized nodules were visualized by staining the fixed cultures with Alizarin red−S, and the stain was extracted with 10% cetylpyridinium chloride to quantify mineralization colorimetrically (OD at 595 nm) [19].

2.3.3. 3′,5′-Cyclic adenosine monophosphate (cAMP) ELISA

BMSCs were seeded into 12-well plates (8×10^4/well). Cells were treated with PTH (1–34) (100 nM) or PTX (3 nM), and incubated for 0-, 5-, 15-, 3-, 60- and 90 min. At the end of incubation, culture media was removed, and cAMP level in the lysates was determined by an ELISA (Cayman Co., Ann Arbor, MI, USA) following the manufacturer's protocol. Total protein in each well was determined by Micro-BCA (Pierce, Rockford, IL, USA) to normalize cAMP data [20].

2.4. In vivo studies

2.4.1. Pharmacokinetics of PTX

The pharmacokinetic study was carried out in virgin adult female New Zealand rabbits ($n = 6$ in each group). Animals were acclimatized for a few days and given ad libitum access to food and water throughout the experimental period unless stated otherwise. The daily oral dose of PTX in human is 21 mg/kg/day and when converted based on body surface area, rabbit dose comes to 75 mg/kg/day [21,22]. Prior PTX dosing, rabbits were fasted for 12–14 h and the drug was administered orally at 12.5-, 25- and 75 mg/kg doses as suspension. Blood was drawn from the marginal ear vein into heparinized microfuge tubes at 0.083-, 0.25-, 0.5-, 1.0-, 1.5-, 2.0-, 4.0-, 6.0-, 8.0-, 10.0 and 24.0 h post-dose. Plasma was harvested and stored at −70 ± 10 °C until analysis.

100 μl plasma was extracted with ethyl acetate and the supernatant was separated and dried under N_2 in TurboVap. The dried extract was reconstituted in the mobile phase and injected into a column (Bridge Waters; 5 μm, 50 × 4.6 mm id) and analyzed by LC-MS/MS system API 5500 Qtrap (SCIEX, Toronto, Ontario, Canada).

Data acquisition and quantification were performed using Analyst™ (version 1.6.3 software; SCIEX, Toronto, Ontario, Canada) according to the previously published protocol [23,24]. The concentration-time data was subjected to noncompartmental analysis using Phoenix WinNonlin software (version 8.0; Certara Inc., Princeton, NJ, USA) to calculate different pharmacokinetic parameters including volume of distribution (V_d), elimination phase half-life ($t_{1/2}$), and area under the curve (AUC). The observed maximum plasma concentration (C_{max}) and the time to reach the maximum plasma concentration (T_{max}) were obtained by visual inspection of the experimental data. AUC from 0 to T_{last} (AUC_{0-t}) was calculated using the linear trapezoidal rule.

2.4.2. Bone formation in growing rabbits

3-months old (1.5 ± 0.2 kg) female NZW rabbits were treated with

PTX (12.5mg/kg p.o. and 25 mg/kg p.o.) for 30 days. Calcein (20 mg/kg, subcutaneous) was injected 10 days and 24 h before sacrifice. After that femurs of the treated animals were fixed in 70% isopropanol and 60 μm section were made using Isomet-Slow Speed Bone Cutter (Buehler, Lake Bluff, IL) followed by photography using confocal microscope (LSM 510 Meta, Carl Zeiss) with appropriate filters by following our previously published protocol with minor modifications [20]. We measured periosteal perimeters, single-labeled surface (sLS), double-labeled surface (dLS) and interlabeled thickness (IrLTh), and these values were used to calculate mineralizing surface/bone surface (MS/BS), mineral apposition rate (MAR) and bone formation rate BFR as follows: MS/BS = (1/2 sLS + dLS)/BS(%); MAR = IrLTh/10 days (μm/day); BFR/BS = MAR × MS/BS ($\mu m^3/\mu m^2$/day).

2.4.3. Studies in osteopenic rabbits

8-months old (3.5 ± 0.8 kg) female rabbits were bilaterally OVX and left for 90 days to develop osteopenia as per our previous protocol [19]. After successful development of osteopenia, rabbits were divided into the following groups: sham + vehicle (water), Ovx + vehicle, Ovx + PTX (12.5mg/kg by oral gavage) and Ovx + PTH (20 μg/kg s.c.) [19] (n = 8/group). For dosing, the required amount of PTX was dissolved in 1 ml water and the same volume of water was used as the vehicle. All treatments were given for four months. Calcein (20 mg/kg, subcutaneous) was injected twice before sacrificing at 10-days interval [19].

Blood was collected at the time of recruitment (BL), after the development of osteopenia (0 month), mid-point of treatment (2 months), and end point of treatment (4 months) to assess bone turnover markers.

2.4.4. μCT analysis

Micro-computed tomography (μCT) analysis of excised bones was carried out using the SkyScan1076 CT scanner (Aartselaar, Belgium). Rabbit bone scanning was performed at 18 μm pixel size, using X-ray source 86 kV, 110 mA. Reconstruction was carried out on a modified Feldkamp algorithm using the SkyScan NRecon software. Projections were obtained over an angular range of 180°. Image slices were reconstructed using the cone-beam reconstruction software version 2.6 based on the Feldkamp algorithm (SkyScan). All analyses were performed using CTAn software, SkyScan. For femur trabecular analysis, 100 slices were selected, leaving 50 slices from the start of the growth plate as a reference point. For cortical analysis, 100 slices were selected, leaving 500 slices from the start of the growth plate as a reference point. For BMD calculation two different density phantom rods were used for calibration; a low- and a high-density phantom rod had BMD values of 0.25 g-hydroxyapatite (HA)/cm^3 and 0.75 g-HA/cm^3 respectively. Attenuation coefficient was calculated for each phantom rod using μCT where low- and high-density phantom rods had attenuation coefficients of 0.01784 and 0.02438, respectively. Bone mineral content (BMC) was calculated using the formula BMC = BMD × bone volume (VOI). Both BMD and VOI were calculated using the CTAn software [19].

2.4.5. Ex vivo mineralization

At the end of treatments osteoblast differentiation was assessed by inducing mineralization as described in Section 2.3.2.

2.4.6. Bone turnover markers

Serum cross-linked C-telopeptide of type I collagen (CTX−I) and serum procollagen type I N-terminal propeptide (PINP) levels were determined by ELISA (MyBioSource, USA.) following the manufacturer's protocols.

2.4.7. qPCR

RNA was extracted from proximal femurs using the trizol extraction method. cDNA was synthesized with RevertAid cDNA synthesis kit (Fermentas, Austin, USA) using 2 μg total RNA. SYBR green chemistry was employed to perform to quantify mRNA levels of various genes using a Light Cycler 480 (Roche Molecular Biochemicals, Indianapolis, USA) [25]. Table 1 lists all primer pairs used in the study. Hypoxanthine-guanine phosphoribosyltransferase (HPRT) was used as internal control.

Table 1
Primer sequences of various genes used for qPCR.

Gene name	Primer sequence	Accession no.
RunX2	F-GAGAGCTCAGCCGGGAAT R-GAGTGGCTGCAGGCTAGG	NM_017345159.1
Col 1	F-CCTATTGGGAGCCGAGGT R-CAGGTTCACCCTTGTTTCCA	NM_001195668.1
TRAP	F-CCGTTCACTCCAGAACGTG R-GTTGCCAATGTGGTCGTG	NM_001081988.1
RANK	F-GAGGGACAGCCTCCTCGTAT R-GAAGGCCACCACCAGAAC	NM_008261434.2
OPG	F-GAAAGGCATCTTTGCACCAG R-TTCTTCCTGCTGCTCCAACT	NM_001099964.2
RANKL	F-TGGAAGGTTCATGGTTCGAT R-GTGCAAAAGGCTGAGTTTCA	NM_002712966.3
HPRT	F-GCTTTCCTTGGTCAAGCAGT R-CACTTCGAGGGGTCCTTTTC	NM_001105671.1

2.4.8. L5 compression test

We followed a previously described protocol [19] with some modifications. Briefly, L5 vertebra was isolated, completely cleaned of muscle and ligament and frozen at -20 °C until the compression test was performed using a Universal Testing Machine (SSTM-25, United Calibration Corporation, CA, USA). L5 height was 20 mm and displacement rate was 0.5 mm/min. DATUM Material Testing Software, version 5 was used for data acquisition and processing. The load-displacement curves were used to calculate ultimate load (N), energy to fracture (N-mm), stiffness (N/mm) and Young's modulus (N/mm^2) according to the previously published protocol [19]. Regression analysis was performed by GraphPad Prism 5 software to determine the correlation between maximum load and BMC [26].

2.4.9. Histomorphometry of trabecular bone

Femurs were fixed in 70% isopropanol and 60 μm sections were made using Isomet-Slow Speed Bone Cutter (Buehler, Lake Bluff, IL) followed by photography using a confocal microscope (LSM 510 Meta, Carl Zeiss, Inc., Thornwood, NY). MS/BS, MAR) and BFR/BS were calculated as described in Section 2.4.2 [19,27].

2.4.10. Tartrate-resistant acid phosphatase (TRAP) staining

For TRAP histochemistry, decalcified femur metaphyses were fixed in 4% paraformaldehyde and dehydrated in graded ethanol. Wax blocks were prepared and bones were sectioned at 6 μm thickness. The sections were stained by pararosaniline chloride and naphthol AS-BI phosphate according to our previously published protocol [28]. The development of red color intensity is proportional to TRAP activity. After TRAP staining, osteoclast number (N.Oc) was calculated using Bioquant Osteo software and normalized by total bone surface (BS) (Bioquant image analysis, USA).

2.4.11. Determination of calcium weight in bones

We used a modified protocol of a previously published report for this determination [29]. We took three reference materials (carbon, aluminium and hydroxyapatite) on single stub and imaged them in backscattered (BE) mode in FEI ESEM Quanta 200 in order to set the contrast and brightness such that the grayscale values of the reference materials fall near the low and high ends of grey level dynamic range for calibration. Rabbit femur bones from the metaphysis region were embedded in plastic resin and 60 μm sections were made using Isomet-Slow Speed Bone Cutter. After optimization of BE grey level values for

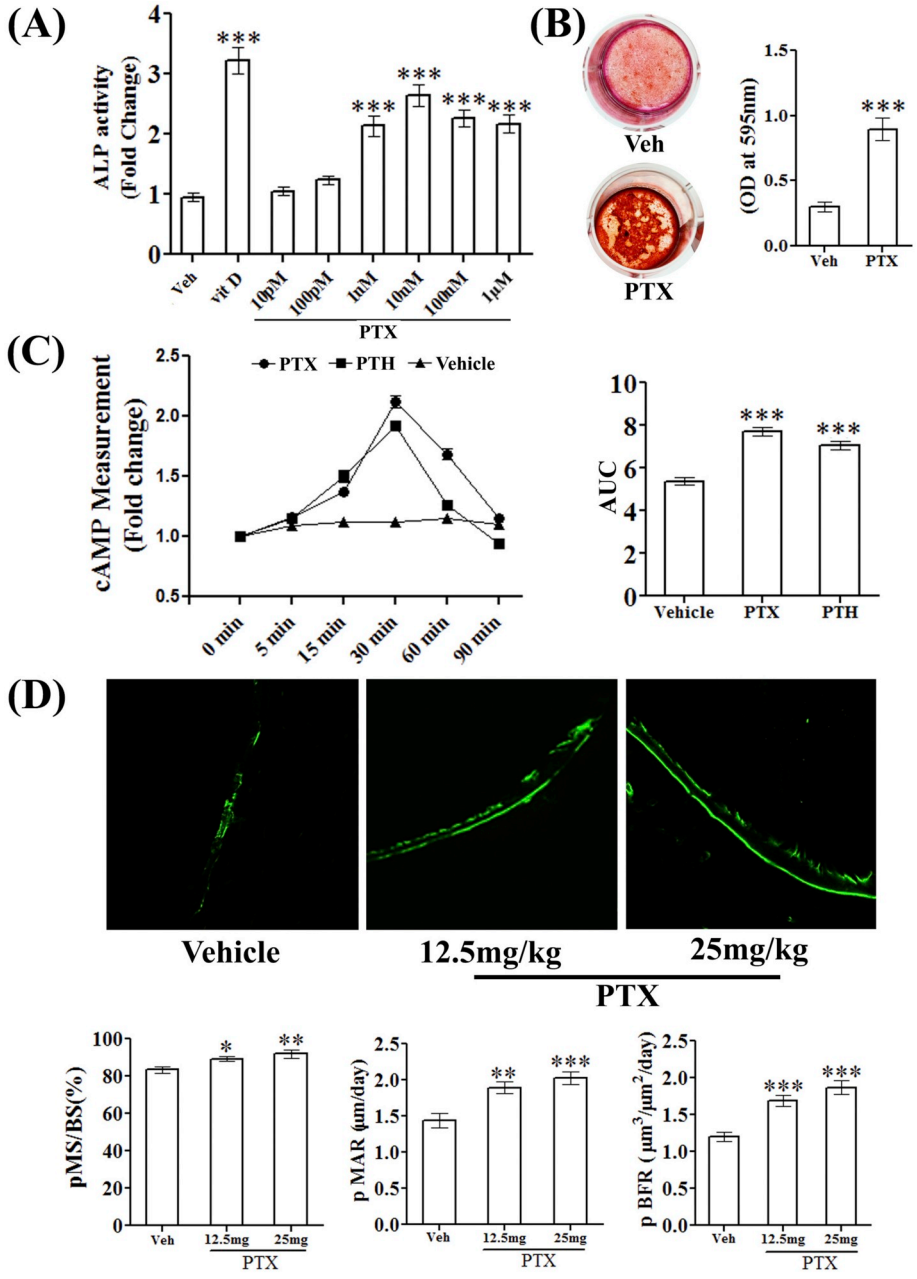

Fig. 1. PTX has an osteogenic effect. (A) Rabbit BMSC (4×10^4 cells/well) were treated with PTX for 48 h at indicated concentrations and ALP (alkaline phosphatase) activity was determined. (B) At the determined EC_{50}, nodule formation in BMSC was assessed. (C) Intracellular cAMP in BMSC was assessed by ELISA in response to PTX and PTH. (D) 3-months old growing female NZW rabbits were orally dosed daily with PTX (12.5 mg/kg and 25 mg/kg) and through time-spaced calcein labeling protocol, surface referent bone formation parameters at femur mid-diaphysis were measured as described in Materials and methods. pMS/BS, periosteal-mineralizing surface per bone surface; pMAR, periosteal mineral apposition rate; pBFR/BS, periosteal bone formation rate. Vehicle (veh) group was administered 1 ml water/day. Data represented as mean ± SEM, $n = 8$/group. For all in vitro experiments, $n = 3$; $^*p < 0.05$, $^{**}p < 0.01$, $^{***}p < 0.001$ compared to vehicle.

Table 2
Pharmacokinetic parameters of PTX.

Parameters	12.5 mg/Kg	25 mg/Kg	75 mg/Kg
Maximum concentration [C_{max} (ng/ml)]	572.33 ± 145.31	3413.33 ± 1523.95	8043.33 ± 1358.84
Maximum concentration [C_{max} (nM/ml)]	2.05 ± 0.522	12.26 ± 5.4	28.89 ± 4.87
Time req. for maximum concentration [t_{max} (h)]	1.00	0.83 ± 0.29	1.17 ± 0.29
Half-life [$T_{1/2}$ (h)]	3.35 ± 0.60	3.31 ± 0.26	3.07 ± 0.49
Total concentration [$AUC_{0\text{-}t}$ (ng h/ml)]	1377.55 ± 318.56	6638.94 ± 295.04	24,255.81 ± 8025.51
Total concentration $AUC_{0\text{-}\infty}$ (ng h/ml)	1385.05 ± 319.80	6707.70 ± 299.29	24,383.68 ± 8197.47
Clearance/F (L/h/kg)	9.38 ± 2.32	3.73 ± 0.16	3.32 ± 1.11

all the reference materials, bone sections were scanned at the same contrast, brightness, and magnification. The micrographs were acquired and analyzed for BE grey level value in Image J software by randomly taking three 1000 X 1000 μm^2 area from each micrograph to calculate BE values. Thus obtained BE values were plotted against the atomic number of the reference materials. For calculating calcium percentage in bone sections, the equation used was [y = 0.199x − 4.982; y = weight of calcium, x = BE grey level value] considering calcium in HA to be 39.8% and pure carbon to be 0%.

2.4.12. Determination of bone crystallinity

Rabbit femur metaphyses were embedded in plastic resin and 60 μm sections were made using Isomet-Slow Speed Bone Cutter. These sections were subjected to X-ray diffraction using a PAN analytical X'Pert

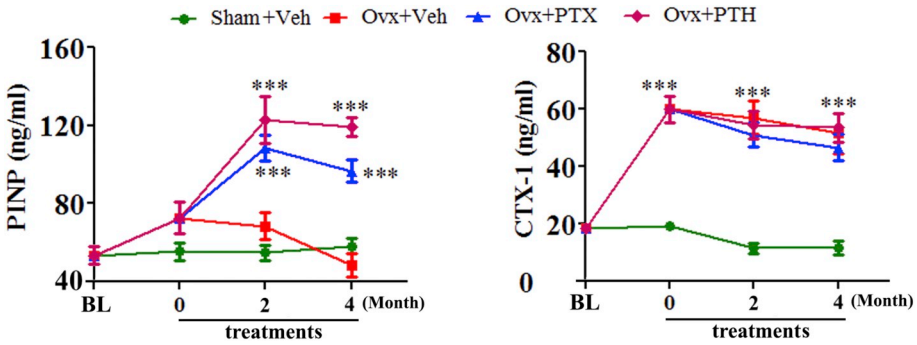

Fig. 2. PTX selectively increases serum osteogenic marker in osteopenic rabbits. Serum PINP (A) and CTX-1 (B) levels were determined by respective ELISA kits at baseline (before OVX), 0 day (3 months after OVX and start of the treatments), 2 months post-treatment and 4 months post-treatment. Data represented as mean ± SEM, $n = 8$/group. $^{**}p < 0.01$, $^{***}p < 0.001$ compared to respective baseline (BL) values.

Pro X-ray diffractometer (Rigaku Smartlab ® HRXRD). Cu Kα monochromatic radiation was used with operating parameters of 40 kV voltages and 30 mA current. The XRD patterns were recorded between 10° to 80° (2θ) in step of 0.010 intervals with 1 s counting time at each step. The crystal size was calculated by Scherer Equation (nm) measured at relative intensities (cps) by comparing it with JCPDS- 00-009-432. FWHM was calculated from the average of three highest XRD peaks in the region of HA ranging from 23.8 to 59° θ [19].

2.5. Statistical analyses

Data were expressed as the mean ± standard error of the mean (SEM). Statistical differences among the different treatment groups were analyzed by one-way ANOVA followed by a post hoc Dunnett's multiple comparison tests of significance using GraphPad Prism 5. The levels of statistical significance in comparison to sham (control) group has been indicated by p values (< 0.05, < 0.01 and < 0.001) in the figure legend. Data having two groups were assessed by t-test to evaluate the statistical difference.

3. Results

3.1. Dose determination of PTX

Rabbit BMSCs were treated with PTX (10 pM–1 μM) and osteoblast differentiation was assessed by ALP assay. Data showed a significant increase ($p < 0.001$) in ALP activity by PTX with an EC_{50} of 3.07 ± 1.37 nM (Fig. 1A). At the EC_{50} concentration, PTX significantly enhanced ($p < 0.001$) mineralized nodule formation in BMSC (Fig. 1B). At this concentration, PTX also stimulated ($p < 0.001$) intracellular cAMP in BMSC that was comparable to PTH (Fig. 1C).

We next carried out pharmacokinetic (PK) studies to determine the minimum oral PTX dose required to achieve the plasma PTX levels to the range of osteogenic EC_{50} determined in vitro. PK studies were carried out at three oral doses; 75 mg/kg (equivalent to adult human dose), 25 mg/kg and 12.5 mg/kg. Maximum serum concentration (C_{max}) of PTX at 12.5mg/kg dose was 2.05 ± 0.522 nM which was close to the osteogenic EC_{50} (Table 2). Furthermore, when growing rabbits were dosed with 12.5- and 25 mg/kg PTX for 4 wk., the cortical bone formation parameters (periosteal (p-) mineralizing surface, mineral accrual rate, and bone formation rate) were increased over the vehicle group (Fig. 1D). Because, PTX at 12.5- and 25 mg/kg doses showed comparable osteogenic effect, the 12.5mg/kg dose was selected as the minimum effective dose and used in all subsequent studies.

3.2. PTX selectively increases serum osteogenic marker in osteopenic rabbit

Serum bone turnover markers were measured at baseline (at the time of recruitment), 3 months post-OVX (treatment start point), and 2- and 4-months after various treatments (Fig. 2). Serum PINP was not different between sham and OVX + veh at all-time points. PTX and PTH increased ($p < 0.001$) serum PINP over sham at 2- and 4 months post treatments (Fig. 2).

Post-OVX, serum CTX-1 was robustly increased ($p < 0.001$) in all groups compared to sham at all time-points. These data indicated a selective osteoanabolic effect of PTX similar to PTH (Fig. 2).

3.3. PTX restores femur trabecular and cortical bones in osteopenic rabbits

At the endpoint, significant loss of BMD and deterioration of micro-architecture were observed in the proximal femur metaphysis of OVX + veh compared to sham ($p < 0.01$). PTX completely restored all the parameters up to the level of the sham. PTH also restored all parameters to the level of sham, however, Tb.Th was significantly higher ($p < 0.05$) than the sham group (Fig. 3A).

All groups had comparable BMD at femur mid-diaphysis. Cs.Th was significantly decreased ($p < 0.05$) in OVX + veh compared to sham. PTX treatment completely restored Cs.Th and this effect was comparable with PTH. Endosteal perimeter and cortical porosity were higher ($p < 0.05$) in osteopenic animals and PTX treatment failed to restore these parameters (Fig. 3B).

3.4. PTX restores vertebral trabecular bones and compressive strength in osteopenic rabbits

Since lumbar vertebrae bear the weight of the upper body and undergo BMD loss in post-menopausal women [30] we took the 5th lumbar vertebra for our study. At the end point significant loss of BMD ($p < 0.001$), BMC ($p < 0.01$) and deterioration of micro-architecture were observed in L5 vertebra of OVX + veh compared to sham. Both PTX and PTH restored all trabecular parameters to the level of sham (Fig. 4A).

In comparison to the sham group, compressive load bearing capacity ($p < 0.05$), energy to failure ($p < 0.05$) and stiffness ($p < 0.01$) of L5 were reduced in the OVX group, and treatment of OVX rabbits with PTX or PTH completely restored these parameters to the levels of the sham group (Fig. 4B). Young's modulus (or modulus of elasticity) is a measure of the ability of a material/bone to withstand changes in deformation under compression. In osteopenic rabbits, Young's modulus of L5 decreased significantly ($p < 0.05$), and both PTX and PTH restored it to the sham level thus suggesting restoration of vertebral elasticity by these treatments (Fig. 4B). There was a strong correlation between the BMC and maximum load at L5 ($r^2 = 0.8974$), and the slope and intercept of the regression line was similar in all groups (Fig. 4C).

3.5. PTX is osteogenic but not anti-osteoclastogenic

At the end of the treatments, ex vivo nodule formation was studied using BMSCs harvested from femurs. OVX + Veh group showed reduced ($p < 0.05$) nodule formation compared to sham whereas both drugs increased ($p < 0.001$) nodule formation over the sham (Fig. 5A).

At the transcript levels, Runx2 (the osteoblast transcription factor) was decreased ($p < 0.01$) in the OVX femurs compared to sham whereas PTX and PTH increased ($p < 0.001$) Runx2 expression by > 2-

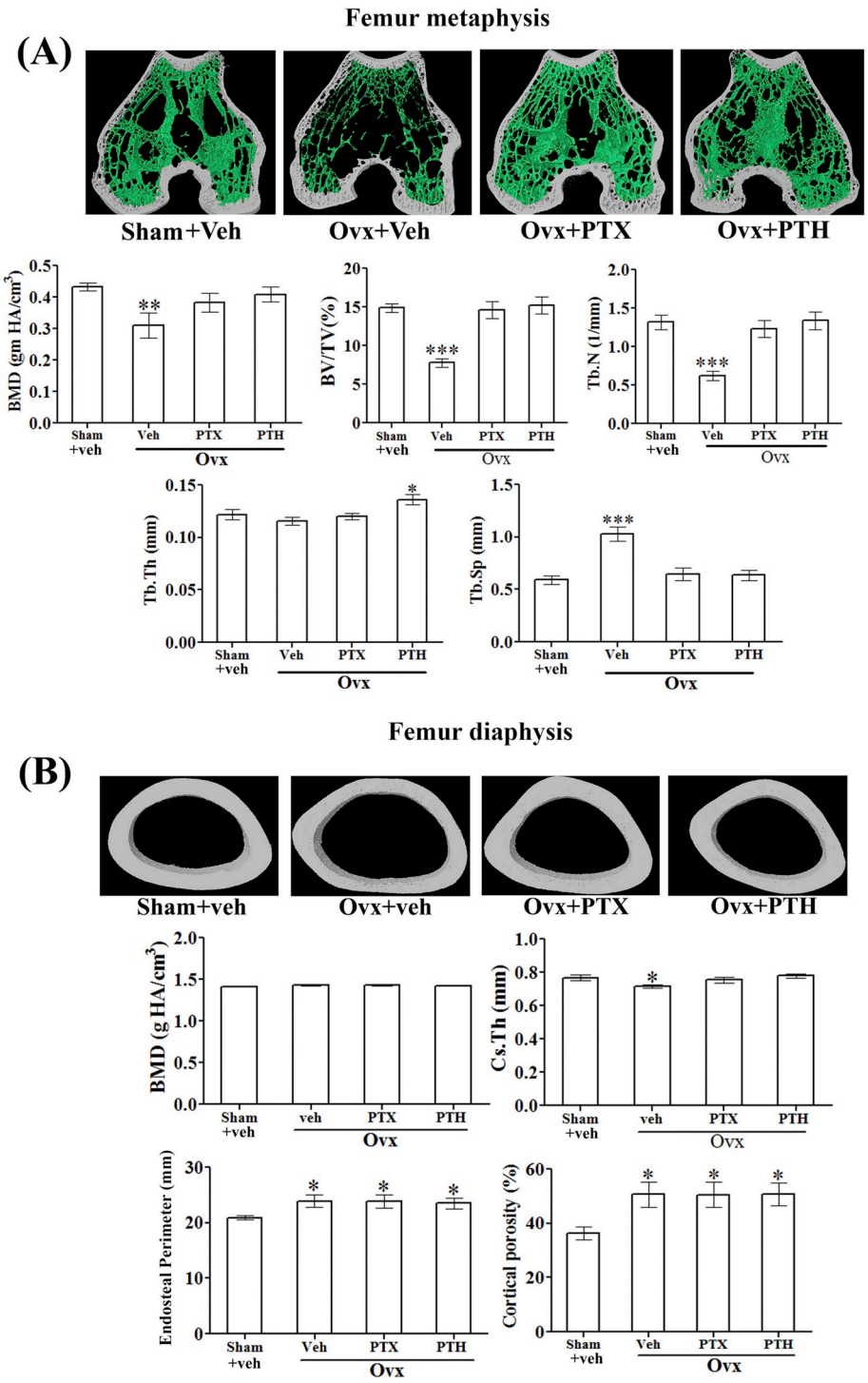

Fig. 3. PTX restored both trabecular and cortical bone mass and microarchitecture in osteopenic OVX rabbits. (A) Various trabecular parameters at femur proximal metaphysis were determined by μCT. Representative μCT images in various groups are shown in the upper panel and calculated parameters are shown in the lower panels. BMD, bone mineral density; BV/TV, bone volume per tissue volume; Tb.N, trabecular number; Tb.Th, trabecular thickness; Tb.sp., trabecular spacing. (B) Various cortical parameters at femur diaphysis were determined by μCT. Representative μCT images in various groups are shown in the upper panel and calculated parameters are shown in the lower panels. Cs.Th, cross-sectional thickness. Data represented as mean ± SEM, $n = 8$/group; $^{*}p < 0.05$, $^{**}p < 0.01$ and $^{***}p < 0.001$ compared to sham.

folds. mRNA level of another osteogenic gene, type 1 collagen was decreased ($p < 0.001$) in OVX + veh compared to sham and both drugs restored this transcript to the sham level. On the other hand, the expression of osteoclastogenic genes including the RANKL/OPG ratio, TRAP, and RANK was increased ($p < 0.001$) in OVX + veh compared to sham and neither drug altered the OVX-induced changes (Fig. 5B). Consistent with the increased osteoclastogenic genes in OVX bones, femur sections showed increased ($p < 0.001$) TRAP stained regions and the number of osteoclast per bone surface (N.Oc/BS) in the OVX + veh group compared to sham. PTX or PTH treatment had no effect on OVX-induced rise in N.Oc (Fig. 5C).

We next confirmed the osteogenic effect of PTX by measuring bone surface referent parameters at the trabecular site of femur metaphysis. OVX + veh group showed decreased MS/BS ($p < 0.05$), MAR ($p < 0.001$) and BFR ($p < 0.001$) compared to sham. All surface referent bone formation parameters were comparable between sham, PTX and PTH groups (Fig. 5D).

3.6. PTX improves bone quality in osteopenic rabbits

Bone crystallinity was assessed by XRD-based FWHM. Higher FWHM reflects lower crystallinity and thus indicates poor crystal packing. FWHM values in the femurs of OVX + vehicle group were significantly higher ($p < 0.05$) than the sham and both PTX and PTH

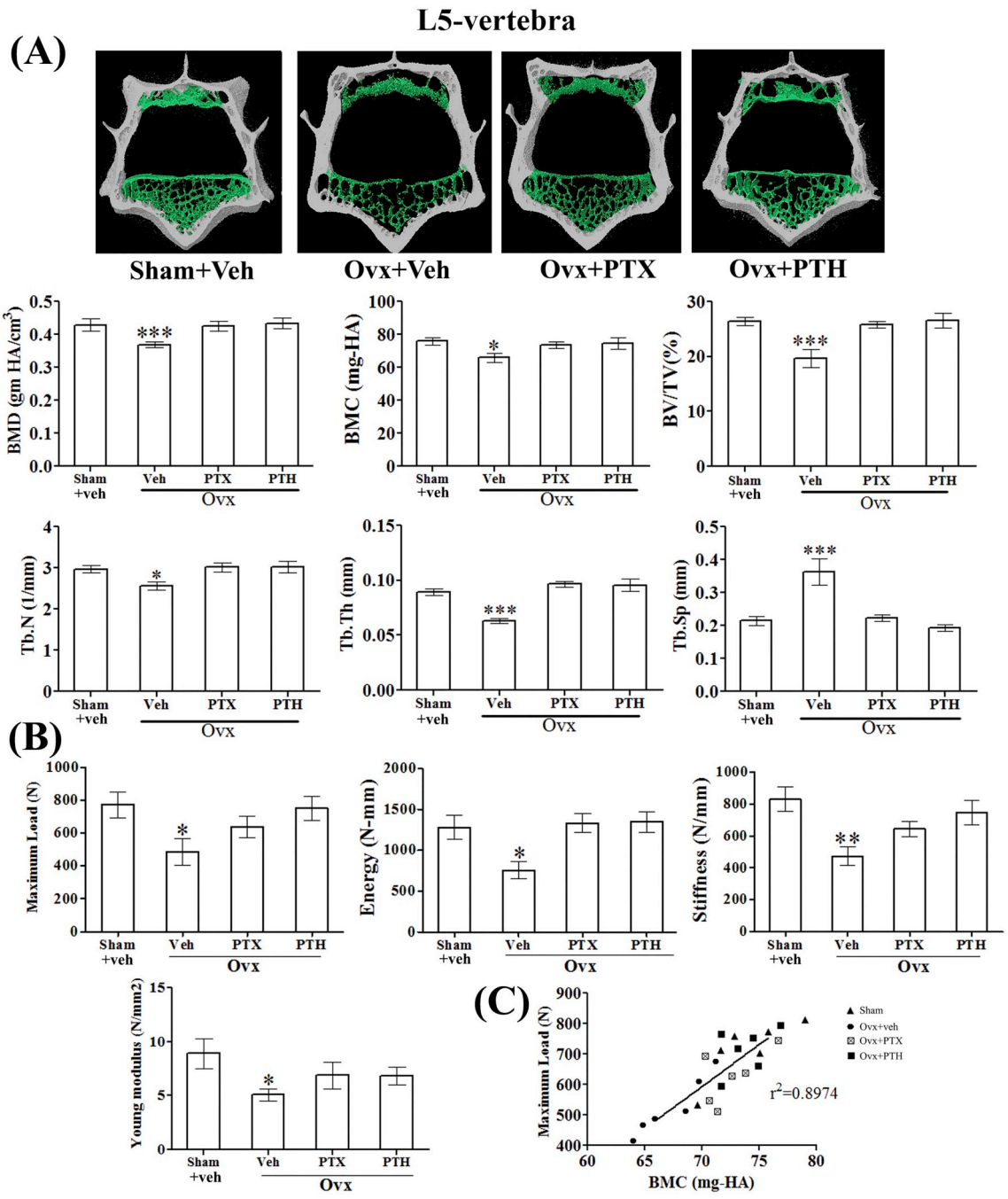

Fig. 4. PTX restored trabecular bone mass, microarchitecture, and strength of L5 vertebra of osteopenic OVX rabbits. (A) Various trabecular parameters at L5 were determined by μCT. Representative μCT images in various groups are shown in the upper panel and calculated parameters are shown in the lower panels. (B) Compressive bone strength and elasticity in L5 were determined by the protocols described in the Materials and methods. (C) Linear regression analyses were performed across various groups between BMC and maximum load at L5. The coefficient of determinant (r^2) is indicated on the graph. Data represented as mean ± SE, $n = 8$/group. *$p < 0.05$, **$p < 0.01$ and ***$p < 0.001$ compared to sham.

decreased it (Fig. 6A).

Next, we measured calcium weight percentage in the sections of femur metaphysis by BE mode and found that OVX + veh group has significantly lesser ($p < 0.01$) calcium weight than the sham group (Fig. 6B). Strikingly, both PTX and PTH groups had significantly increased ($p < 0.001$) tissue calcium weight than sham (Fig. 6B).

4. Discussion

The current study demonstrates a significant bone anabolic effect of PTX in osteopenic rabbits. PTX at 1/6th of the adult human oral dose given to OVX osteopenic rabbits mimicked all of the skeletal effects of PTH administration. PTX, at this dose, increased bone mass, microarchitecture, strength, and quality. There are no oral osteoanabolic drugs. PTH (1–34) and a PTHrP peptide analog are administered by daily injection. Alternative delivery of PTH (1–34) by oral, transdermal or nasally have met with limited success [31]. Long-Term treatment of osteoporosis with improved patient compliance likely requires oral over parenteral administration. For example, calcilytics, small molecules which are oral extracellular calcium-sensing receptor antagonists, cause a transient increase in PTH secretion but have been found to lack an osteogenic effect in phase II clinical trials [32,33]. Our current findings

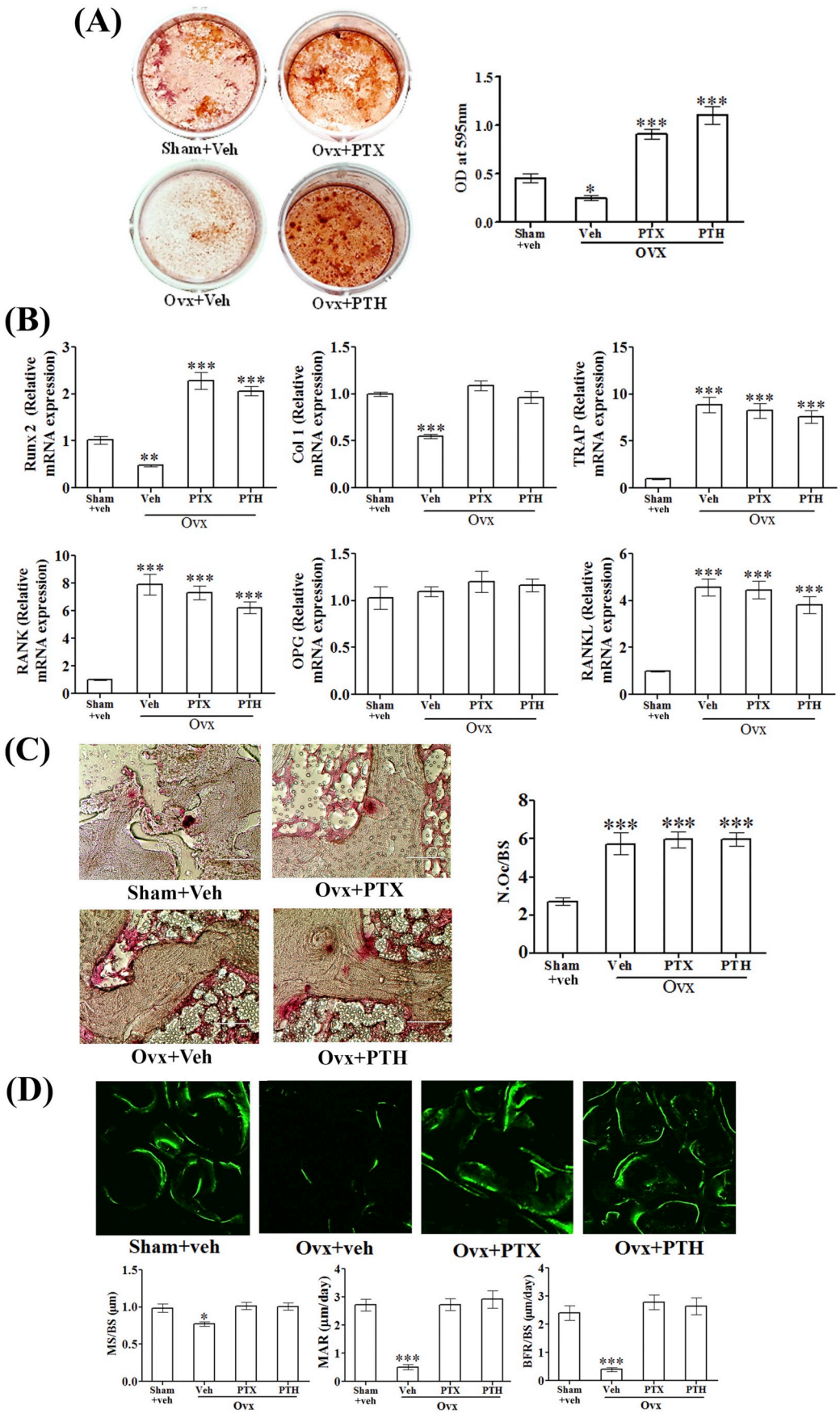

Fig. 5. PTX promotes bone formation in OVX osteopenic rabbits without affecting resorption. (A) BMSC from rabbits of indicated groups was harvested as described in Fig. 1A. Left panel showing mineralized nodules and right panel showing quantification after dye extraction as described in the Materials and methods. (B) Total RNA was isolated from femur trabecular region devoid of marrow and qPCR was performed using gene-specific primers described in Table 1. Data expressed after normalization with HPRT mRNA. (C) Left panel showing TRAP stained images of different treatment groups at 40× magnification. Right panel showing osteoclast number (N.Oc./BS) determined from the stained images. (D) Surface referent bone formation at distal femur metaphysis was determined by time-spaced calcein labeling of bones. The upper panel showing representative micrographs of bone sections and the lower panel showing quantification using Bioquant software. Data represented as mean ± SEM, $n = 6$/group; $^{*}p < 0.05$, $^{**}p < 0.01$ and $^{***}p < 0.001$ compared to sham.

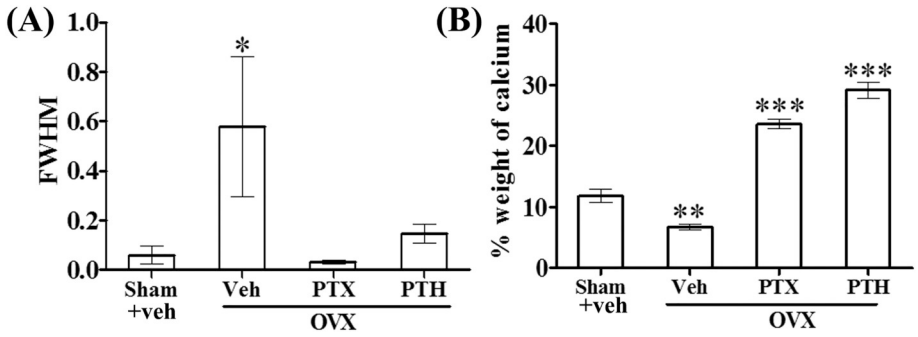

Fig. 6. PTX treatment favorably alters bone biomaterial in OVX osteopenic rabbits. (A) Crystalinity of powdered bone samples (femur metaphysis) of indicated groups was determined by XRD as described in the Materials and methods. (B) Back-scattered EM was used on the sections of femur metaphysis of indicated groups to determine calcium weight. Data represented as mean ± SEM, $n = 6$; $^{*}p < 0.05$, $^{**}p < 0.01$ and $^{***}p < 0.001$ compared to sham.

suggest PTX, at the appropriate oral dose, may be used as an osteoanabolic drug.

The osteogenic concentration of PTX determined from ALP assay on rabbit BMSC was achieved at a dose of 12.5 mg/kg, which was 1/6th the dose used clinically [22]. At this dose, PTX enhanced modeling-directed bone growth in growing animals and completely restored bone mass, microarchitecture, strength, quality and material property in OVX rabbits to sham levels. We observed decreased PTX clearance at the higher doses, suggesting non-linearity in elimination, which is consistent with earlier reports on the oral clearance of PTX [21] and theophylline (a methylxanthine drug) [34]. The skeletal effect of PTX in OVX rabbits was comparable to PTH, suggesting to us that PTX manifested a clear osteoanabolic effect. Indeed, PTX mimicked some of the hallmarks of PTH, including the stimulation of serum PINP without altering the OVX-induced rise in serum CTX-1. PTX increased surface referent bone formation parameters, restored both L5 bone mass and elasticity and increased cortical thickness with no effect on OVX-induced increases in cortical porosity. Increases in the ex vivo nodule formation of BMSC, tissue osteogenic genes and the RANKL/OPG ratio by PTX to the levels of the PTH treated group, suggested to us a similar molecular response by these two drugs.

Restoration of bone mass accounts for only 40% of fracture risk, whereas microarchitecture and material properties constitute the remaining risk [35]. In rabbits, we and others have shown that PTH increases bone mass and strength with an attendant increase in elasticity and mineral heterogeneity [19,36]. The effects of PTH were replicated in the current study, and PTX mimicked the effects of PTH to result in complete restoration of bone mass, architecture, and strength. Material tensile strain increases FWHM, while the relaxation of tensile strain decreases it [37]. We observed increased FWHM in OVX compared to sham animals, which was decreased by PTX treatment. Tissue calcium levels in both PTX- and PTH-treated rabbits were significantly higher than the sham values, likely because of the new bone formation induced by these treatments. The combination of higher tissue calcium and lower FWHM in PTX- and PTH-treated rabbits appeared to have conferred greater stiffness, an important strength parameter.

Our study addressed for the first time several critical issues pertaining to the anabolic effect of PTX. Firstly, the effect was achieved by the oral administration of PTX, which is more widely practiced clinically instead of parenteral routes of administration used in previous preclinical studies with this drug [12] [14]. Secondly, we determined the drug dose empirically from oral bioavailability data suggested by it's in vitro osteogenic EC_{50} to generate an osteogenic dose in vivo which was 1/6th of the human oral dose. Such a low dose of PTX affording an osteogenic effect comparable to PTH is likely to be safe for long-term treatment, as required for post-menopausal osteoporosis. Thirdly, the anabolic effect was observed in rabbits, a species having Haversian remodeling, thus making our findings relevant to the bone remodeling characteristics of primates as opposed to previous studies in rats and mice, which have no active Haversian remodeling. Indeed, commencing PTX treatment after the development of osteopenia (therapeutic mode) made our observations relevant to the clinical setting. Finally, evidence of bone restoration included not only bone mass but also strength and material quality. Others have shown PTX dosing at the human equivalent dose for 8 weeks in OVX osteopenic rats with femur osteotomy gave a trend of improved femoral bone strength which was not significant [13]. While we observed PTX significantly enhanced the serum osteogenic marker PINP at 2 months, translating this response to enhanced bone strength might require longer drug treatment. Indeed, treatment with PTX in OVX rats for 3 months generated a significant osteogenic effect (S. Pal, N. Chattopadhyay; Unpublished observations).

The current study does have limitations. The withdrawal of PTH has been reported to maintain distal femoral bone mass for 8 weeks in OVX rats [38] and up to 12 months in post-menopausal women, when femur neck and spine BMD were assessed [39]. We did not investigate the effect of discontinuation of PTX to determine the time required for osteopenia to reappear in the OVX animals, so we cannot comment on whether a substantial drug-free time is possible with PTX. Fracture healing is impaired in the osteopenic condition, but we have not yet determined if PTX can enhance fracture healing in this condition. Nor have we studied cortical bone formation in OVX rabbits at the periosteal, intra-cortical and endocortical compartments. Given that modulation of cAMP and cGMP signaling regulates blood pressure [40] and blood flow [41] and PTH is a vasodilator which increases bone blood flow [42] it will be important to determine whether PTX improves bone perfusion in OVX rabbits. Large variations in lumbar compressive strength parameters have been reported for adult female NZW rabbits [26,43,44]. Although the levels of change in these parameters between the sham and OVX groups of the present study were similar to our previous report [19] however their absolute values differed considerably between these two studies. Whether variations in tissue processing, age at the time of sacrifice and L5 trabecular bone volume between these two studies (the present and [19]) contributed to such difference remained unexplained. Other indicators of bone material properties such as the mineral-to-matrix ratio, phosphate-to-carbonate substitution and collagen cross-links [45] with respect to bone strength have not been assessed in the current study.

Nevertheless, the current study clearly demonstrates a significant bone anabolic effect on PTX in osteopenic rabbits. Discovery and development of new drugs take an enormous amount of time, money and effort, and the effort can be bottlenecked at the clinical trial stage. It is crucial to find strategies to improve the success rate of getting drugs to the clinic. Drug repurposing is one such strategy, and generally refers to

studying a well-characterized drug known to treat one condition or disease to see if it is safe and effective for treating other diseases which in this case is post-menopausal osteoporosis [46,47]. We have demonstrated that PTX at 1/6th of the adult human dose given to OVX osteopenic rabbits mimicked all the skeletal effects of PTH including restoration of bone mass, microarchitecture, strength, and quality. Clearly, assessment of the efficacy of PTX in post-menopausal osteoporosis as an orally active osteoanabolic drug is warranted.

Acknowledgments

The authors are thankful for the technical assistance provided by Kavita Singh at the confocal facility of the Electron Microscopy Unit, Sophisticated Analytical Instrument Facility (SAIF), CSIR-CDRI, Lucknow, India.

Supporting grants

Council of Scientific and Industrial Research, India.

Disclosures

The authors have no conflict of interest.

References

[1] P. Andreopoulou, R.S. Bockman, Management of postmenopausal osteoporosis, Annu. Rev. Med. 66 (2015) 329–342.
[2] M. Luz Rentero, C. Carbonell, M. Casillas, M. Gonzalez Bejar, R. Berenguer, Risk factors for osteoporosis and fractures in postmenopausal women between 50 and 65 years of age in a primary care setting in Spain: a questionnaire, Open Rheumatol J 2 (2008) 58–63.
[3] S.A. Polyzos, P. Makras, Z. Efstathiadou, A.D. Anastasilakis, Investigational parathyroid hormone receptor analogs for the treatment of osteoporosis, Expert Opin. Investig. Drugs 24 (2) (2015) 145–157.
[4] A. Modi, S. Sajjan, R. Insinga, J. Weaver, E.M. Lewiecki, S.T. Harris, Frequency of discontinuation of injectable osteoporosis therapies in US patients over 2 years, Osteoporos. Int. 28 (4) (2017) 1355–1363.
[5] W.C. Huang, C.Y. Chen, S.J. Lin, C.S. Chang, Medication adherence to oral anticancer drugs: systematic review, Expert. Rev. Anticancer. Ther. 16 (4) (2016) 423–432.
[6] B.C. Silva, J.P. Bilezikian, Parathyroid hormone: anabolic and catabolic actions on the skeleton, Curr. Opin. Pharmacol. 22 (2015) 41–50.
[7] T. Fujita, T. Meguro, R. Fukuyama, H. Nakamuta, M. Koida, New signaling pathway for parathyroid hormone and cyclic AMP action on extracellular-regulated kinase and cell proliferation in bone cells. Checkpoint of modulation by cyclic AMP, J. Biol. Chem. 277 (25) (2002) 22191–22200.
[8] R.E. Moore, C.K. Smith 2nd, C.S. Bailey, E.F. Voelkel, A.H. Tashjian Jr., Characterization of beta-adrenergic receptors on rat and human osteoblast-like cells and demonstration that beta-receptor agonists can stimulate bone resorption in organ culture, Bone Miner 23 (3) (1993) 301–315.
[9] T.K. Sampath, P. Simic, R. Sendak, N. Draca, A.E. Bowe, S. O'Brien, S.C. Schiavi, J.M. McPherson, S. Vukicevic, Thyroid-stimulating hormone restores bone volume, microarchitecture, and strength in aged ovariectomized rats, J. Bone Miner. Res. 22 (6) (2007) 849–859.
[10] E.S. Cho, J.H. Yu, M.S. Kim, M. Yim, Rolipram, a phosphodiesterase 4 inhibitor, stimulates inducible cAMP early repressor expression in osteoblasts, Yonsei Med. J. 46 (1) (2005) 149–154.
[11] M.F. McCarty, J.H. O'Keefe, J.J. DiNicolantonio, Pentoxifylline for vascular health: a brief review of the literature, Open Heart 3 (1) (2016) e000365.
[12] G. Cakmak, M.S. Sahin, B.H. Ozdemir, E. Karadenlz, Effect of pentoxifylline on healing of segmental bone defects and angiogenesis, Acta Orthop. Traumatol. Turc. 49 (6) (2015) 676–682.
[13] M.M. Vashghani Farahani, R. Ahadi, M. Abdollahifar, M. Bayat, The effects of pentoxifylline adminstration on fracture healing in a postmenopausal osteoporotic rat model, Lab Anim Res 33 (1) (2017) 15–23.
[14] T. Kinoshita, S. Kobayashi, S. Ebara, Y. Yoshimura, H. Horiuchi, T. Tsutsumimoto, S. Wakabayashi, K. Takaoka, Phosphodiesterase inhibitors, pentoxifylline and rolipram, increase bone mass mainly by promoting bone formation in normal mice, Bone 27 (6) (2000) 811–817.
[15] S. Champion, N. Lapidus, G. Cherie, V. Spagnoli, J. Oliary, A.C. Solal, Pentoxifylline in heart failure: a meta-analysis of clinical trials, Cardiovasc. Ther. 32 (4) (2014) 159–162.
[16] L. Baofeng, Y. Zhi, C. Bei, M. Guolin, Y. Qingshui, L. Jian, Characterization of a rabbit osteoporosis model induced by ovariectomy and glucocorticoid, Acta Orthop. 81 (3) (2010) 396–401.
[17] V. Gilsanz, T.F. Roe, D.T. Gibbens, E.E. Schulz, M.E. Carlson, O. Gonzalez, M.I. Boechat, Effect of sex steroids on peak bone density of growing rabbits, Am. J. Phys. 255 (4 Pt 1) (1988) E416–E421.
[18] S. Castaneda, R. Largo, E. Calvo, F. Rodriguez-Salvanes, M.E. Marcos, M. Diaz-Curiel, G. Herrero-Beaumont, Bone mineral measurements of subchondral and trabecular bone in healthy and osteoporotic rabbits, Skelet. Radiol. 35 (1) (2006) 34–41.
[19] M.P. Khan, A.K. Singh, P. Shrivastava, M.C. Tiwari, G.K. Nagar, H.K. Bora, V. Parameswaran, S. Sanyal, J.R. Bellare, N. Chattopadhyay, Odanacatib restores trabecular bone of skeletally mature female rabbits with osteopenia but induces brittleness of cortical bone: a comparative study of the investigational drug with PTH, estrogen, and alendronate, J. Bone Miner. Res. 31 (3) (2016) 615–629.
[20] S. Pal, K. Khan, S.P. China, M. Mittal, K. Porwal, R. Shrivastava, I. Taneja, Z. Hossain, D. Mandalapu, J.R. Gayen, M. Wahajuddin, V.L. Sharma, A.K. Trivedi, S. Sanyal, S. Bhadauria, M.M. Godbole, S.K. Gupta, N. Chattopadhyay, Theophylline, a methylxanthine drug induces osteopenia and alters calciotropic hormones, and prophylactic vitamin D treatment protects against these changes in rats, Toxicol. Appl. Pharmacol. 295 (2016) 12–25.
[21] B.M. Best, J.C. Burns, J. DeVincenzo, S.J. Phelps, J.L. Blumer, J.T. Wilson, E.V. Capparelli, J.D. Connor, Pharmacokinetic and tolerability assessment of a pediatric oral formulation of pentoxifylline in kawasaki disease, Curr Ther Res Clin Exp 64 (2) (2003) 96–115.
[22] J.E. Frampton, R.N. Brogden, Pentoxifylline (oxpentifylline). A review of its therapeutic efficacy in the management of peripheral vascular and cerebrovascular disorders, Drugs Aging 7 (6) (1995) 480–503.
[23] K.S. Moola, B.S.R. Challa, C.K. Bannoth, Quantification of tolvaptan in rabbit plasma by LC-MS/MS: application to a pharmacokinetic study, J Pharm Anal 5 (6) (2015) 371–377.
[24] B. Davies, T. Morris, Physiological parameters in laboratory animals and humans, Pharm. Res. 10 (7) (1993) 1093–1095.
[25] J.K. Tripathi, S. Pal, B. Awasthi, A. Kumar, A. Tandon, K. Mitra, N. Chattopadhyay, J.K. Ghosh, Variants of self-assembling peptide, KLD-12 that show both rapid fracture healing and antimicrobial properties, Biomaterials 56 (2015) 92–103.
[26] B.L. Pennypacker, L.T. Duong, T.E. Cusick, P.J. Masarachia, M.A. Gentile, J.Y. Gauthier, W.C. Black, B.B. Scott, R. Samadfam, S.Y. Smith, D.B. Kimmel, Cathepsin K inhibitors prevent bone loss in estrogen-deficient rabbits, J. Bone Miner. Res. 26 (2) (2011) 252–262.
[27] K. Hara, M. Kobayashi, Y. Akiyama, Vitamin K2 (menatetrenone) inhibits bone loss induced by prednisolone partly through enhancement of bone formation in rats, Bone 31 (5) (2002) 575–581.
[28] K. Khan, A. Singh, M. Mittal, K. Sharan, N. Singh, P. Dixit, S. Sanyal, R. Maurya, N. Chattopadhyay, [6]-Gingerol induces bone loss in ovary intact adult mice and augments osteoclast function via the transient receptor potential vanilloid 1 channel, Mol. Nutr. Food Res. 56 (12) (2012) 1860–1873.
[29] P. Roschger, P. Fratzl, J. Eschberger, K. Klaushofer, Validation of quantitative backscattered electron imaging for the measurement of mineral density distribution in human bone biopsies, Bone 23 (4) (1998) 319–326.
[30] J.S. Finkelstein, S.E. Brockwell, V. Mehta, G.A. Greendale, M.R. Sowers, B. Ettinger, J.C. Lo, J.M. Johnston, J.A. Cauley, M.E. Danielson, R.M. Neer, Bone mineral density changes during the menopause transition in a multiethnic cohort of women, J. Clin. Endocrinol. Metab. 93 (3) (2008) 861–868.
[31] P. Morley, Delivery of parathyroid hormone for the treatment of osteoporosis, Expert Opin Drug Deliv 2 (6) (2005) 993–1002.
[32] S. Kumar, C.J. Matheny, S.J. Hoffman, R.W. Marquis, M. Schultz, X. Liang, J.A. Vasko, G.B. Stroup, V.R. Vaden, H. Haley, J. Fox, E.G. DelMar, E.F. Nemeth, A.M. Lago, J.F. Callahan, P. Bhatnagar, W.F. Huffman, M. Gowen, B. Yi, T.M. Danoff, L.A. Fitzpatrick, An orally active calcium-sensing receptor antagonist that transiently increases plasma concentrations of PTH and stimulates bone formation, Bone 46 (2) (2010) 534–542.
[33] F. Cosman, N. Gilchrist, M. McClung, J. Foldes, T. de Villiers, A. Santora, A. Leung, S. Samanta, N. Heyden, J.P. McGinnis 2nd, E. Rosenberg, A.E. Denker, A phase 2 study of MK-5442, a calcium-sensing receptor antagonist, in postmenopausal women with osteoporosis after long-term use of oral bisphosphonates, Osteoporos. Int. 27 (1) (2016) 377–386.
[34] L.J. Lesko, Dose-dependent kinetics of theophylline, J. Allergy Clin. Immunol. 78 (4 Pt 2) (1986) 723–727.
[35] H. Fonseca, D. Moreira-Goncalves, H.J. Coriolano, J.A. Duarte, Bone quality: the determinants of bone strength and fragility, Sports Med. 44 (1) (2014) 37–53.
[36] R. Aleksyniene, J.S. Thomsen, H. Eckardt, K.G. Bundgaard, M. Lind, I. Hvid, Parathyroid hormone PTH(1-34) increases the volume, mineral content, and mechanical properties of regenerated mineralizing tissue after distraction osteogenesis in rabbits, Acta Orthop. 80 (6) (2009) 716–723.
[37] E.P. Paschalis, D.B. Burr, R. Mendelsohn, J.M. Hock, A.L. Boskey, Bone mineral and collagen quality in humeri of ovariectomized cynomolgus monkeys given rhPTH(1-34) for 18 months, J. Bone Miner. Res. 18 (4) (2003) 769–775.
[38] J.M. Hock, Anabolic actions of PTH in the skeletons of animals, J. Musculoskelet. Neuronal Interact. 2 (1) (2001) 33–47.
[39] B.Z. Leder, R.M. Neer, J.J. Wyland, H.W. Lee, S.M. Burnett-Bowie, J.S. Finkelstein, Effects of teriparatide treatment and discontinuation in postmenopausal women and eugonadal men with osteoporosis, J. Clin. Endocrinol. Metab. 94 (8) (2009) 2915–2921.
[40] R. Feil, B. Kemp-Harper, cGMP signalling: from bench to bedside. Conference on cGMP generators, effectors and therapeutic implications, EMBO Rep. 7 (2) (2006) 149–153.

[41] P.K. Pang, H.F. Janssen, J.A. Yee, Effects of synthetic parathyroid hormone on vascular beds of dogs, Pharmacology 21 (3) (1980) 213–222.
[42] H.H. Wang, E.D. Drugge, Y.C. Yen, M.R. Blumenthal, P.K. Pang, Effects of synthetic parathyroid hormone on hemodynamics and regional blood flows, Eur. J. Pharmacol. 97 (3–4) (1984) 209–215.
[43] X. Liu, W. Lei, Z. Wu, Y. Cui, B. Han, S. Fu, C. Jiang, Effects of glucocorticoid on BMD, micro-architecture and biomechanics of cancellous and cortical bone mass in OVX rabbits, Med. Eng. Phys. 34 (1) (2012) 2–8.
[44] B. Grardel, B. Sutter, B. Flautre, E. Viguier, F. Lavaste, P. Hardouin, Effects of glucocorticoids on skeletal growth in rabbits evaluated by dual-photon absorptiometry, microscopic connectivity and vertebral compressive strength, Osteoporos. Int. 4 (4) (1994) 204–210.
[45] E.P. Paschalis, R. Mendelsohn, A.L. Boskey, Infrared assessment of bone quality: a review, Clin. Orthop. Relat. Res. 469 (8) (2011) 2170–2178.
[46] S. Pushpakom, F. Iorio, P.A. Eyers, K.J. Escott, S. Hopper, A. Wells, A. Doig, T. Guilliams, J. Latimer, C. McNamee, A. Norris, P. Sanseau, D. Cavalla, M. Pirmohamed, Drug repurposing: progress, challenges and recommendations, Nat. Rev. Drug Discov. 18 (2019) 41–58.
[47] S.M. Corsello, J.A. Bittker, Z. Liu, J. Gould, P. McCarren, J.E. Hirschman, S.E. Johnston, A. Vrcic, B. Wong, M. Khan, J. Asiedu, R. Narayan, C.C. Mader, A. Subramanian, T.R. Golub, The drug repurposing hub: a next-generation drug library and information resource, Nat. Med. 23 (4) (2017) 405–408.